Strategies for the development of three dimensional scaffolds from piezoelectric poly(vinylidene fluoride)

D. M. Correia[1,2], C. Ribeiro[1,], V. Sencadas[1,3], L. Vikingsson[4], M. Oliver Gasch[5], J. L. Gómez Ribelles[4, 5] G. Botelho[2], S. Lanceros-Méndez[1,*]*

[1]Centro/Departamento de Física da Universidade do Minho, Campus de Gualtar, 4710-057 Braga, Portugal

[2]Centro/Departamento de Química, Universidade do Minho, Campus de Gualtar, 4710-057 Braga, Portugal

[3]School of Mechanical, Materials and Mechatronics Engineering, University of Wollongong, Wollongong, NSW 2522, Australia

[4]Centre for Biomaterials and Tissue Engineering (CBIT), Universitat Politècnica de València, Camino de Vera s/n, 46022 Valencia, Spain.

[5]Biomedical Research Networking Center in Bioengineering, Biomaterials and Nanomedicine (CIBER-BBN), Valencia, Spain.

***Corresponding Authors: cribeiro@fisica.uminho.pt; lanceros@fisica.uminho.pt; Tel.: +351 253604320; Fax: +351 253604061**

KEYWORDS: poly(vinylidene fluoride); scaffolds; tissue engineering; mechanical properties; piezoelectric.

Abstract

Cell supports based on electroactive materials, that generate electrical signal variations as a response to mechanical deformations and vice-versa, are gaining increasing attention for tissue engineering applications. In particular, poly(vinylidene fluoride), PVDF, has been proven to be suitable for these applications in the form of films and two-dimensional membranes. In this work, several strategies have been implemented in order to develop PVDF three-dimensional scaffolds. Three processing methods, including solvent casting with particulate leaching and three-dimensional nylon, and freeze extraction with poly(vinyl alcohol) templates are presented in order to obtain three-dimensional scaffolds with different architectures and interconnected porosity. Further, it is shown that the scaffolds are in the electroactive β-phase and show a crystallinity degree of ~ 45 %. Finally, quasi-static mechanical measurements showed that an increase of the porous size within the scaffold leads to a tensile strengths and the Young's modulus decrease, allowing tuning scaffold properties for specific tissues.

Introduction

Different processing techniques are being applied to tailor the shape of the scaffolds for temporary or permanent cell supports in tissue engineering (TE) applications [1-2]. The versatility of these scaffolds is associated with variables such as composition, size and shape, degree of porosity and pore size, that can be modeled to obtain an optimized system for specific cells and/or tissues [3]. These natural or synthetic functional scaffolds are used for culturing cells in order to generate tissues that can be later implanted in the human body [2].

Strong efforts are being performed in the development of three dimensional (3D) scaffolds as support for tissue engineering applications. They offer important advantages comparatively to two dimensional (2D) structures such as, films and fiber mats, as they allow a biomimetic environment for cell-cell interaction, cell migration and morphogenesis, promoting a better interconnection between cells and tissues [4]. In this sense, the scaffolds should present a pore size enabling the accommodation of cells, promoting/allowing cellular adhesion, growth and migration. Furthermore, a suitable pore interconnectivity is essential for the transport of nutrients and metabolites [4], as well as, an appropriate microenvironment, allowing the transmission of biochemical and/or mechanical and/or electrical clues.

Several methods have been proposed for 3D scaffolds production, conventional methods including etching, template-assisted synthesis, solvent casting, particulate leaching, gas foaming, contact printing, wet-chemical approach and electrospinning [4-5]. More recently, rapid prototyping (RP) technologies including fused deposition modeling (FDM), precision extrusion deposition (PED), selective laser sintering (SLS), stereolithography (STL) and 3D printing have been used to overcome the drawbacks of conventional methods, including inaccurate control over the micro- and macro-scale features, allowing the fabrication of scaffolds with a controlled microstructure and porosity [6].

Three-dimensional structures based on smart and functional biomaterials are increasingly playing an important role in TE applications once they do not work just as passive supports, but can also play a relevant role in the development of tissues and cells [7] by triggering/stimulating specific cues on both cells and tissues [8]. Also, in order to promote a better compatibility between cells and the biomaterial, different strategies have been used, including surface tailoring with bio-mimetic molecules such as peptides and adhesive proteins, tuning chemical and physical

properties to produce similarity to native extra-cellular matrix (ECM), to modulate the surface and bulk properties or providing external therapeutic molecules in order to stimulate the surrounding cells and tissues [8]. The internal modulation mainly involves biomimetic modification of chemical, physical and/or biological properties in order to mimic the native tissue and provide a more friendly environment and enhance target functions such as adhesion, proliferation, migration and differentiation [8]. Among the most interesting clues to be provided to specific cells, such as mechanical [9] and (bio)chemical [10], electrical clues have already proven to be important in TE applications [11, 12]. In that sense, piezoelectric polymers, materials that generate a voltage under mechanical loading without the need of electrodes or external power source, offer a unique opportunity to deliver electrical cues directly to cells [13]. The relevance of this effect for biomedical applications is that several tissues such as bone, cannot only take advantage of this effect, as they are subjected to electromechanical functions, but they are piezoelectric themselves [14], suggesting the biomimetic need of this effect in the scaffold. Previous studies have shown that electroactive polymers, in particular piezoelectric poly(vinylidene fluoride) (PVDF), are suitable for the development of electro-mechanically bioactive supports [15-16].

PVDF is a semi-crystalline polymer that can crystallize in at least four crystalline polymorphs, namely α, β, δ and γ, being the β-phase the one with the highest piezoelectric response [17-19]. Further, it is biocompatible, allowing its use in biomedical applications [7, 18, 20].

Different techniques have been used to process PVDF and its polymer/composites based in different strategies (**Table 1**) to obtain various morphologies including micropillars [21], particles [20, 22], films [23-25] and fibers [15, 26-31] in order to better suit specific tissue

engineering strategies. Further, it has been shown that substrates based on PVDF have different influence on cell adhesion, proliferation and differentiation [7] depending on their morphology. Table 1 summarizes the different PVDF structures used as supports for cell viability studies. To the best of our knowledge no studies regarding 3D structures based on piezoelectric materials and, in particular, in PVDF have been reported in the literature.

Thus, in order to extend the applicability of the material for effective tissue engineering applications, this work reports on three different strategies for the preparation of electroactive 3D PVDF scaffolds with tailored porosity and pore size. Further, the influence of the processing technique on polymer porosity, electroactive phase, crystallinity and mechanical properties, were systematically studied.

Experimental section

Materials

Poly(vinylidene fluoride) (PVDF) (Solef 1010/1001) was acquired from Solvay. Analytical grade N,N-Dimethylformamide (DMF) was purchased from Merck and formic acid and ethanol were purchased from Sigma Aldrich. Poly (vinyl alcohol) (PVA) filaments with 1.75 mm were supplied by Plastic2Print (Netherlands). Sodium chloride, 99% was purchased from Fisher Scientific.

Scaffolds production methods

Solvent-casting particulate leaching

PVDF scaffolds were prepared via solvent casting method. The polymer was dissolved in a DMF solution (10 % w/v) under mechanical stirring. After complete dissolution of PVDF, 5, 10 and 20 g of NaCl was added to the solution. After solvent evaporation at room temperature, the membranes were placed under vacuum and allow drying at room temperature. After solvent evaporation, the membranes were washed thoroughly with distilled water until complete salt removal. The resultant microporous membranes were again vacuum dried, until a constant weight was obtained.

Solvent casting with a 3D nylon template

For this procedure, nylon plates (Saatilon) with a pore diameter of 60 and 150 μm (NT-60 and NT-150) were cut into $2 \times 2\ cm^2$ samples and piled up on top of each other (5 layers) inside a Teflon Petri dish. The PVDF solution (prepared as indicated above) was carefully added to the nylon plate assembly. After solvent evaporation at room temperature, the scaffolds were rinsed with formic acid to remove the nylon plates in order to obtain the porous scaffold. Finally, the scaffolds were rinsed with water and dried in the same conditions as the solvent casting samples reported above.

Freeze extraction with a 3D PVA template

PVA templates were fabricated in the 3D printer Bits from Bytes 3D Touch. The printer parameters were optimized to obtain different porous structures. Four PVA templates with different filament distances were fabricated. The designation of each template is presented in **table 2**.

PVDF scaffolds were produced by two different approaches. The PVDF solution (prepared as indicated above) was casted into a PVA template to completely fill the porous structure. Afterwards, DMF solvent evaporation was performed at 60 ºC in a Homo Vacuo-Temp. After complete solvent evaporation, the PVA template was extracted with deionized water in order to obtain the porous structure in the form of interconnected channels. The PVA washing step was performed 3 times daily during 3 days. Furthermore, a freeze extraction method was used to prepare highly porous scaffolds. After introducing the PVDF solution into the free space of the PVA template, it was quickly frozen by immersion in liquid nitrogen and then stored at -80 ºC to induce crystallization and phase separation between PVDF and DMF. Then, ethanol precooled at -80 ºC was poured on top of the template containing the frozen polymer solution in order to extract DMF while the whole system is kept at -80 ºC. The ethanol was changed twice a day during 3 days to fully remove the DMF solvent. After solvent removal, the PVA template was extracted by washing repeatedly with deionized water at room temperature, as described above.

Figure 1 schematizes the procedures used for the PVDF three dimensional scaffolds production.

A neat porous PVDF membrane (10 % w/v in DMF) prepared via solvent casting [37] method was used to compare with the tridimensional structures.

Sample characterization

PVDF scaffolds morphology and porosity distribution were analyzed by scanning electron microscopy with a Scanning Electron Microscope (SEM), Quanta 650, from FEI with an accelerating voltage of 5 kV and by a Binocular *LEICA MZ APO*. The analyzed samples were

previously coated with a thin gold layer using a sputter coating (Polaron, model SC502). Pore size distribution was examined by ImageJ software.

The crystalline phase or phases present in the scaffolds were confirmed by Fourier transform infrared spectroscopy performed at room temperature in a JASCO 4100 apparatus in ATR mode from 4000 to 400 cm^{-1} using 64 scans at a resolution of 4 cm^{-1}. Differential scanning calorimetry measurements (DSC) were performed in a Mettler Toledo 823e apparatus using a heating rate of 10 $ºC.min^{-1}$ under a nitrogen purge.

Mechanical experiments were performed on cylindrical samples with approximately 6 mm diameter and 3 mm height in a Shimadzu AG-IS universal testing machine in compression mode at a test velocity of 1 $mm.min^{-1}$. The samples were submitted to a compressive-strain cycle load up to 10 cycles at a strain of 15% with a 500 N load cell. Strain deformation was measured by machine cross-head displacement. The Young's modulus was calculated from the slope at the initial linear stage of the stress–strain curves and the tensile strength was determined from the maximum load.

The porosity of the PVDF scaffolds was measured by liquid displacement method using a pycnometer. The weight of the pycnometer filled with ethanol (Merck), as a non-solvent of PVDF, was measured and labeled as W_1; the PVDF scaffolds, whose weight was W_s, were immersed in ethanol. After the sample was saturated by ethanol, additional ethanol was added to complete the volume of the pycnometer. Then, the pycnometer was weighted and labeled as W_2; the sample filled with ethanol was then taken out of the pycnometer [38]. The residual weight of

the ethanol and the pycnometer was labeled W_3. The porosity of the membranes was calculated according to **equation 1**:

$$\varepsilon = \frac{W_2 - W_3 - W_S}{W_1 - W_3} \quad (1)$$

The mean porosity of each membrane was obtained as the average of the values determined in three samples [39].

Results and discussion

Morphology

In order to produce piezoelectric PVDF scaffolds, the polymer was dissolved in DMF solvent and different strategies were applied to tailor the final porosity and pore interconnectivity of the polymer structures. The PVDF scaffold obtained through solvent casting with NaCl as a sacrificial material (**figure 2**a) shows a porous structure with the bigger porous with approximately 300 - 400 μm (**figure 3**a), which are of the same size range as pristine NaCl crystals (262 to 370 μm). The porous formation occurs after polymer crystallization in places previously occupied by the porogen, and the pore size is controlled by the size of the sacrificial particle size. However, the salt leaching method does not allow the design of structures with completely interconnected pores with a regular and reproducible morphology.

Tridimensional PVDF structures with high porosity and interconnected pores can be achieved by solvent casting with a 3D nylon template and freeze extraction with a PVA template (figure 2b and 2c). As shown in figure 2b and 2c, scaffolds fabricated using a 3D nylon template present a

good interconnected porous structure (figure 2c) with well distributed pores. When nylon templates were used porous structures with approximately 60 μm and 130 μm can be obtained (figure 2b and 3b). The size of the pores was governed by the sacrificial filament geometry and the space between the filaments was fully filled with the polymer solution. Then, crystallization leads to small interconnected porous (below 5 μm) within the major ones (figure 2c), corresponding to the former filament places. The samples prepared by freeze drying extraction show the pores left by the sacrificial PVA filaments, with an inner diameter between 300 – 400 μm (figure 2c).

The same procedure was not feasible when a PVA template obtained by 3D printing was used, due to the larger diameter of the PVA filaments. Further, even increasing the solvent temperature during solvent evaporation to 60 ºC, followed by the dissolution of PVA in water, it was not possible to achieve a tridimensional porous structure (results not shown). To overcome this issue, the solution was immersed in liquid nitrogen to immediately freeze the solution and stored at -80 ºC with ethanol, to improve the DMF solvent dissolution by the ethanol, while the polymer chains remained frozen (figure 2d). After the samples were washed with water to PVA removal and dried at room temperature, the space initially occupied by the non-solvent became micropores and the pore architecture finally obtained consists in an orthotropic structure of interconnected channels whose walls are in turn connected by micropores. Figure 3c shows that the channels in the scaffolds are well interconnected and their average diameter ranging between 316 and 413 μm corresponds to the diameter of the sacrificial PVA filament obtained by 3D printing (Table 1).

The influence of the adopted processing technique and the porogen used on the overall porosity was assessed by gravimetric method and applying equation 1, while the pore size and its distribution was measured through the SEM images (figure 2). In general, all samples show pores in the same range of the sacrificial material used (figure 3). The highest overall porosity was achieved for the samples with NaCl as porogen, being the sample with the highest porosity the ones with the highest amount of sacrificial material (figure 3).

Polymer phase content

FTIR-ATR spectroscopy was performed in order to study possible chemical modifications induced by the processing technique in the PVDF scaffolds. Moreover, this method provides valuable information to distinguish between the different PVDF polymorphs [17] and, in particular, to quantify the piezoelectric β-phase content present in the scaffolds.

Figure 4a shows the main absorption band at 840 cm^{-1} characteristic of the β-phase of PVDF [17]. Also absorption bands at 765, 795 and 855 cm^{-1}, relative to α-PVDF are also observed, independently of the processing technique. Further, no absorption bands corresponding to the different porogen materials or solvents were detected, which suggests that the removal of the sacrificial materials was complete.

PVDF electroactive β-phase is dominant when the solvent evaporation occurs bellow 70 ºC [17]. Assuming that only α- and β-phase are present, the fraction of β-phase was calculated using **equation 2** [17].

$$F(\beta) = \frac{A_\beta}{\left(\frac{K_\beta}{K_\alpha}\right) A_\alpha + A_\beta} \quad (2)$$

where $F(\beta)$ represents the β-phase content, K_α and K_β the absorption coefficient for each phase and A_α and A_β the absorbance at 766 and 840 cm^{-1}, respectively. The absorption coefficient value is 7.7×10^4 $cm^2.mol^{-1}$ and 6.1×10^4 $cm^2.mol^{-1}$ for K_β *and* K_α, respectively [17].

Figure 4b shows that the scaffolds production methods does not influence significantly the amount of β-phase content. Comparatively to PVDF membranes which present a β-phase content of 91%, scaffolds produced by salt leaching, solvent casting and freeze extraction show β-phase contents of 86, 90 and 94%, respectively. In this sense, as low crystallization temperature (e.g. room temperature) favors the PVDF crystallization in the β-phase, also freeze extraction method induces the formation of the polymer electroactive phase.

The piezoelectric constant of porous samples was measured in our previous studies. From previous works reported from our group it is possible to electrical pole the materials and measure the piezoelectric response (d_{33}) of porous samples [40].

Some toxic solvents such as DMF and formic acid were used during the scaffolds fabrication by three distinct methods. In the solvent casting with NaCl particulate leaching and nylon as a sacrificial material methods, both NaCl salt and nylon was removed only after the completely solvent evaporation with water and formic acid, respectively. The formic acid used to nylon template removal was eliminated with successively water washes. In the freeze extraction method, the DMF was removed by freezing DMF in an ethanol bath. Infrared spectroscopy measurements and DSC, do not present any traces of residual solvents (DMF and formic acid) or sacrificial materials (nylon and PVA) used during the scaffold manufacturing.

The solvent DMF used for PVDF dissolution in the three distinct methods was also used in our other previous studies to obtain scaffolds with different morphologies like fibers and microparticles. For both cytotoxicity studies were performed and results proved that the evaporation of solvent completely occurs once its non-toxic once it's non-inhibit the cell viability like MC3T3-E1 pre-osteoblast [22]. Moreover, cell culturing was performed and the solvent the results demonstrated that PVDF fibers dissolved in DMF solution promotes the cell adhesion, proliferation and differentiation [23].

Thermal characterization

Differential scanning calorimetry (DSC) was performed to assess the influence of the processing technique and porogen in the polymer degree of crystallinity. It was observed that the incorporation of different fillers leads to a shift towards lower temperatures of the melting transition, when compared to the neat PVDF sample obtained from solvent casting, particularly noticed when NaCl is used (**figure 5**). In this way, the strong ionic character of the salt, lead to strong interaction with the highly polar polymer chain, reducing the stability region of the crystalline structure [41]. Moreover, the meting transition appears as a broad endothermic peak for all samples, suggesting a distribution of crystal sizes among the polymer matrix.

The degree of crystallinity (Xc) of the PVDF samples was determined from DSC curves and evaluated by **equation 3** [42].

$$X_c = \frac{\Delta H}{x\Delta H_\alpha + y\Delta H_\beta} \quad (3)$$

where ΔH is the melting enthalpy of the sample; ΔH_α (93.07 Jg^{-1}) and ΔH_β (103.4 Jg^{-1}) are the melting enthalpies of a 100% crystalline sample in the α- and β-phase, respectively, and the x and y the amount of the α- and β-phase present in the sample, calculate through the FTIR results (figure 4) [42].

Different porogen materials show different effects on polymer degree of crystallinity. Pristine PVDF polymer shows a degree of crystallinity ~ 45%, but for the sample prepared with NaCl, the sample shows an X_c around 33%. Low *et al.* [43] showed that when small amounts of NaCl are added to the PVDF solution, the salt, combined with free radicals near the crystalline surface promotes an increase of sample crystallinity [43]. However, beyond a critical concentration, the excess of salt will interact with the PVDF on the crystallite surface and promotes atoms dislocation, resulting in a decrease of the crystallinity degree of the PVDF sample (figure 5b). Most relevant, the large amounts of filler used in the present investigation act as defective structures, leading to hindered spherulite growth during polymer crystallization [17]. On the other hand, when a nylon mesh was used as a template, an increase of the degree of crystallinity of the sample was observed up to 55%, while for the PVDF prepared with PVA porogen, the degree of crystallinity present in the sample is similar to the observed for the pristine PVDF (figure 5b).

Mechanical characterization

Various cellular activities are influenced by mechanical properties of surrounding tissues and scaffolds [44]. Cyclic stress *vs* strain measurements obtained under compressive mode and for a strain of 15%, for the different PVDF structures are shown in **figure 6**. The final mechanical strain of 15% was defined to match the characteristic deformation of the natural cartilage and it is also used as the target strain in experiments with bioreactors for chondrogenic differentiation [45].

The mechanical performance of the scaffolds obtained for different NaCl concentrations show a similar behavior, attributed to the similar porosity (figure 2) present in the sample (data not shown). For all tested samples, the difference between the first and the second cycle is related to the processing history and to the surface of the mechanical pin accommodation among the sample surface. Further, some permanent deformation during the first compression cycle was observed (figure 6). In successive load-unload compression cycles, it was observed an increase of the irreversible processes, leading to permanent deformation, reflected by the slight decrease of the maximum stress reached in the stress-strain loop (figure 6). The samples prepared by nylon template meshes collapse after three consecutive mechanical loading-unloading cycles (data not show), but the maximum stress for the first cycles was quite higher when compared to the rest of the porous samples obtained by different methods. This behavior is probably related to the microstructure and distribution of the pores among the sample, which is characterized by perpendicular channels with an overall porosity of ~ 66 ± 3.3% (figure 3). When the mechanical cycle is applied to the sample, the stress is not uniformly distributed among the polymer bulk due to the dual porosity e.g. small pores of 2 μm diameter and pores with 60 and 150 μm, which leads to a collapse of the channels formed by the nylon mesh, due to the small polymer thickness when compared to the bulk PVDF polymer structure.

For the rest of the samples it was observed that the maximum stress decreases with increasing mechanical loading-unloading cycle, showing the samples obtained from salt leaching and the freeze dried M1 (distance between filaments of 0.6 mm) similar mechanical hysteresis patterns (figure 6). The sample M4 (filaments placed at 1.2 mm between each other) is the one with the lowest maximum stress at the end of each cycle. This behavior is related to the big size of the channels when compared to sample M1 that locally induces a poor mechanical load distribution due to the decrease of the thickness in the region between the channels.

The apparent elastic modulus (E) was calculated from the stress-strain data at 1 % deformation and the results are shown in **table 3**. The scaffolds prepared by NaCl leaching show a higher E when compared to the rest of the samples. This result is interesting due to the high porosity present in these samples, being explained by the fact that the pore walls in such samples are homogeneously distributed among the polymer bulk, which promotes an evenly distribution of the mechanical load between the polymer walls. The samples prepared by PVA template and freeze drying, as well as the ones obtained by nylon mesh show a similar morphology, characterized by the big channels from the template. This leads to a dual distribution of the mechanical stress, one part being supported by the bulk polymer with pore size of ≤ 2 μm and the other by the channels with small wall thickness, which ultimately leads to a decrease of the mechanical properties, as observed in figure 6, and to a decrease of E (table 3).

Thus, **figure 7** shows the PVDF structures with different morphologies and geometries that can be obtained using different processing methods, the PVDF scaffolds with different pore sizes being the ones presented in this work and obtained by three different methods.

Conclusions

PVDF three dimensional scaffolds can be obtained by NaCl salt leaching, solvent casting and freeze extraction with nylon and PVA templates, respectively. The different preparation methods allow tuning pore size, interconnectivity and porosity. Thus, varying the ratio of NaCl / porogen and the distance between the filaments of the templates allows to control the porosity of the scaffold. The structure of the 3D templates allows obtaining scaffolds with well interconnected pores. Infrared spectroscopy showed that all processing methods result in scaffolds mainly in the piezoelectric β-phase of PVDF (between 86 and 94%) and with a degree of crystallinity between 33 and 47%. The characterization of the scaffolds by mechanical compression tests and the relation between scaffold porosity and mechanical properties showed that higher porosities promotes a significant decrease in the tensile strengths and the Young's Modulus, the overall results indicating the suitability of the PVDF scaffolds for tissue engineering applications.

ACKNOWLEDGMENTS

This work is funded by FEDER funds through the "Programa Operacional Fatores de Competitividade – COMPETE" and by national funds arranged by FCT- Fundação para a Ciência e a Tecnologia, project references NANO/NMed-SD/0156/2007, PTDC/CTM-NAN/112574/2009, PEST-C/FIS/UI607/2014 and PEST-C/QUI/UIO686/2013. The authors also thank funding from Matepro –Optimizing Materials and Processes", ref. NORTE-07-0124-FEDER-000037", co-funded by the "Programa Operacional Regional do Norte" (ON.2 – O Novo Norte), under the "Quadro de Referência Estratégico Nacional" (QREN), through the "Fundo Europeu de Desenvolvimento Regional" (FEDER). The authors also thank support from the

COST Action MP1301 “New Generation Biomimetic and Customized Implants for Bone Engineering”. DMC and CR, thank the FCT for the SFRH/BD/82411/2011, SFRH/BPD/90870/2012 grants, respectively. JLGR acknowledges the support of Ministerio de Economía y Competitividad, MINECO, through the MAT2013-46467-C4-1-R project. CIBER-BBN is an initiative funded by the VI National R&D&i Plan 2008-2011, Iniciativa Ingenio 2010, Consolider Program, CIBER Actions and financed by the Instituto de Salud Carlos III with assistance from the European Regional Development Fund.

References

[1] D.M. García Cruz, V. Sardinha, J.L. Escobar Ivirico, J.F. Mano, J.L. Gómez Ribelles, Gelatin microparticles aggregates as three-dimensional scaffolding system in cartilage engineering, J Mater Sci: Mater Med, 24 (2013) 503-513.

[2] A. Seidi, M. Ramalingam, I. Elloumi-Hannachi, S. Ostrovidov, A. Khademhosseini, Gradient biomaterials for soft-to-hard interface tissue engineering, Acta Biomaterialia, 7 (2011) 1441-1451.

[3] M.B. Oliveira, J.F. Mano, Polymer-based microparticles in tissue engineering and regenerative medicine, Biotechnology Progress, 27 (2011) 897-912.

[4] B. Sun, Y.Z. Long, H.D. Zhang, M.M. Li, J.L. Duvail, X.Y. Jiang, H.L. Yin, Advances in three-dimensional nanofibrous macrostructures via electrospinning, Progress in Polymer Science, 39 (2014) 862-890.

[5] C.E. Schmidt, V.R. Shastri, J.P. Vacanti, R. Langer, Stimulation of neurite outgrowth using an electrically conducting polymer, Proceedings of the National Academy of Sciences, 94 (1997) 8948-8953.

[6] D. Rana, S. Arulkumar, A. Vishwakarma, M. Ramalingam, Chapter 10 - Considerations on Designing Scaffold for Tissue Engineering, in: A.V.S.S. Ramalingam (Ed.) Stem Cell Biology and Tissue Engineering in Dental Sciences, Academic Press, Boston, 2015, pp. 133-148.

[7] C. Ribeiro, V. Sencadas, D.M. Correia, S. Lanceros-Méndez, Piezoelectric polymers as biomaterials for tissue engineering applications, Colloids and Surfaces B: Biointerfaces, 136 (2015) 46-55.

[8] R.A. Pérez, J.-E. Won, J.C. Knowles, H.-W. Kim, Naturally and synthetic smart composite biomaterials for tissue regeneration, Advanced Drug Delivery Reviews, 65 (2013) 471-496.

[9] B.P. Chan, K.W. Leong, Scaffolding in tissue engineering: General approaches and tissue-specific considerations, European Spine Journal, 17 (2008) S467-S479.

[10] N.E. Vrana, V. Hasirci, G.B. McGuinness, A. Ndreu-Halili, Cell/tissue microenvironment engineering and monitoring in tissue engineering, regenerative medicine, and in vitro tissue models, BioMed research international, 2014 (2014) 951626.

[11] T.H. Qazi, R. Rai, A.R. Boccaccini, Tissue engineering of electrically responsive tissues using polyaniline based polymers: A review, Biomaterials, 35 (2014) 9068-9086.

[12] J. Pu, C.D. McCaig, L. Cao, Z. Zhao, J.E. Segall, M. Zhao, EGF receptor signalling is essential for electric-field-directed migration of breast cancer cells, Journal of Cell Science, 120 (2007) 3395-3403.

[13] V.V. Kochervinskiĭ, Piezoelectricity in crystallizing ferroelectric polymers: Poly(vinylidene fluoride) and its copolymers (a review), Crystallography Reports, 48 (2003) 649-675.

[14] M.H. Shamos, L.S. Lavine, Piezoelectricity as a Fundamental Property of Biological Tissues, Nature, 213 (1967) 267-269.

[15] H.-F. Guo, Z.-S. Li, S.-W. Dong, W.-J. Chen, L. Deng, Y.-F. Wang, D.-J. Ying, Piezoelectric PU/PVDF electrospun scaffolds for wound healing applications, Colloids and Surfaces B: Biointerfaces, 96 (2012) 29-36.

[16] N. Weber, Y.S. Lee, S. Shanmugasundaram, M. Jaffe, T.L. Arinzeh, Characterization and in vitro cytocompatibility of piezoelectric electrospun scaffolds, Acta Biomaterialia, 6 (2010) 3550-3556.

[17] P. Martins, A.C. Lopes, S. Lanceros-Mendez, Electroactive phases of poly(vinylidene fluoride): Determination, processing and applications, Progress in Polymer Science, 39 (2014) 683-706.

[18] H.G.L. Coster, T.D. Farahani, T.C. Chilcott, Production and characterization of piezo-electric membranes, Desalination, 283 (2011) 52-57.

[19] V. Cauda, G. Canavese, S. Stassi, Nanostructured piezoelectric polymers, Journal of Applied Polymer Science, 132 (2015) 41667.

[20] I.B. Rietveld, K. Kobayashi, H. Yamada, K. Matsushige, Morphology control of poly(vinylidene fluoride) thin film made with electrospray, Journal of Colloid and Interface Science, 298 (2006) 639-651.

[21] J. Xu, M.J. Dapino, D. Gallego-Perez, D. Hansford, Validation and characterization of an acoustic sensor based on PVDF micropillars and patterned electrodes, in: ASME 2010 Conference on Smart Materials, Adaptive Structures and Intelligent Systems, SMASIS 2010, 2010, pp. 451-459.

[22] D.M. Correia, R. Goncalves, C. Ribeiro, V. Sencadas, G. Botelho, J.L.G. Ribelles, S. Lanceros-Mendez, Electrosprayed poly(vinylidene fluoride) microparticles for tissue engineering applications, Rsc Advances, 4 (2014) 33013-33021.

[23] P.M. Martins, S. Ribeiro, C. Ribeiro, V. Sencadas, A.C. Gomes, F.M. Gama, S. Lanceros-Mendez, Effect of poling state and morphology of piezoelectric poly(vinylidene fluoride) membranes for skeletal muscle tissue engineering, Rsc Advances, 3 (2013) 17938-17944.

[24] C. Frias, J. Reis, F. Capela e Silva, J. Potes, J. Simões, A.T. Marques, Polymeric piezoelectric actuator substrate for osteoblast mechanical stimulation, Journal of Biomechanics, 43 (2010) 1061-1066.

[25] J. Reis, C. Frias, C. Canto E Castro, M.L. Botelho, A.T. Marques, J.A.O. Simões, F. Capela E Silva, J. Potes, A new piezoelectric actuator induces bone formation in vivo: A preliminary study, Journal of Biomedicine and Biotechnology, 2012 (2012) 613403.

[26] Z.H. Liu, C.T. Pan, L.W. Lin, H.W. Lai, Piezoelectric properties of PVDF/MWCNT nanofiber using near-field electrospinning, Sensors and Actuators A: Physical, 193 (2013) 13-24.

[27] H. Na, X. Liu, J. Li, Y. Zhao, C. Zhao, X. Yuan, Formation of core/shell ultrafine fibers of PVDF/PC by electrospinning via introduction of PMMA or BTEAC, Polymer, 50 (2009) 6340-6349.

[28] K. Ketpang, J.S. Park, Electrospinning PVDF/PPy/MWCNTs conducting composites, Synthetic Metals, 160 (2010) 1603-1608.

[29] E. Bormashenko, R. Pogreb, Y. Socol, M.H. Itzhaq, V. Streltsov, S. Sutovski, A. Sheshnev, Y. Bormashenko, Polyvinylidene fluoride—piezoelectric polymer for integrated infrared optics applications, Optical Materials, 27 (2004) 429-434.

[30] H. Zhang, J. Zheng, Z. Zhao, C.C. Han, Role of wettability in interfacial polymerization based on PVDF electrospun nanofibrous scaffolds, Journal of Membrane Science, 442 (2013) 124-130.

[31] M. Bhamidipati, B. Sridharan, A.M. Scurto, M.S. Detamore, Subcritical CO2 sintering of microspheres of different polymeric materials to fabricate scaffolds for tissue engineering, Materials Science and Engineering: C, 33 (2013) 4892-4899.

[32] C. Ribeiro, S. Moreira, V. Correia, V. Sencadas, J.G. Rocha, F.M. Gama, J.L. Gomez Ribelles, S. Lanceros-Mendez, Enhanced proliferation of pre-osteoblastic cells by dynamic piezoelectric stimulation, Rsc Advances, 2 (2012) 11504-11509.

[33] Y.K.A. Low, X. Zou, Y.M. Fang, J.L. Wang, W.S. Lin, F.Y.C. Boey, K.W. Ng, beta-Phase poly(vinylidene fluoride) films encouraged more homogeneous cell distribution and more significant deposition of fibronectin towards the cell-material interface compared to alpha-phase poly(vinylidene fluoride) films, Materials science & engineering. C, Materials for biological applications, 34 (2014) 345-353.

[34] Y.S. Lee, G. Collins, T.L. Arinzeh, Ieee, Neural Differentiation of Human Neural Stem/Progenitor Cells on Piezoelectric Scaffolds, in: 2010 IEEE 36th Annual Northeast Bioengineering Conference, 2010.

[35] Y.-S. Lee, G. Collins, T. Livingston Arinzeh, Neurite extension of primary neurons on electrospun piezoelectric scaffolds, Acta Biomaterialia, 7 (2011) 3877-3886.

[36] S.M. Damaraju, S. Wu, M. Jaffe, T.L. Arinzeh, Structural changes in PVDF fibers due to electrospinning and its effect on biological function, Biomedical materials (Bristol, England), 8 (2013) 045007.

[37] J. Nunes-Pereira, S. Ribeiro, C. Ribeiro, C.J. Gombek, F.M. Gama, A.C. Gomes, D.A. Patterson, S. Lanceros-Méndez, Poly(vinylidene fluoride) and copolymers as porous membranes for tissue engineering applications, Polymer Testing, 44 (2015) 234-241.

[38] C.M. Costa, L.C. Rodrigues, V. Sencadas, M.M. Silva, J.G. Rocha, S. Lanceros-Méndez, Effect of degree of porosity on the properties of poly(vinylidene fluoride–trifluorethylene) for Li-ion battery separators, Journal of Membrane Science, 407–408 (2012) 193-201.

[39] Q. Tan, S. Li, J. Ren, C. Chen, Fabrication of Porous Scaffolds with a Controllable Microstructure and Mechanical Properties by Porogen Fusion Technique, International Journal of Molecular Sciences, 12 (2011) 890-904.

[40] V. Sencadas, C. Ribeiro, I.K. Bdikin, A.L. Kholkin, S. Lanceros-Mendez, Local piezoelectric response of single poly(vinylidene fluoride) electrospun fibers, Physica Status Solidi a-Applications and Materials Science, 209 (2012) 2605-2609.

[41] P. Martins, C.M. Costa, M. Benelmekki, G. Botelho, S. Lanceros-Mendez, On the origin of the electroactive poly(vinylidene fluoride) β-phase nucleation by ferrite nanoparticles via surface electrostatic interactions, CrystEngComm, 14 (2012) 2807-2811.

[42] C. Ribeiro, V. Sencadas, J.L.G. Ribelles, S. Lanceros-Méndez, Influence of Processing Conditions on Polymorphism and Nanofiber Morphology of Electroactive Poly(vinylidene fluoride) Electrospun Membranes, Soft Materials, 8 (2010) 274-287.

[43] Y.K.A. Low, L.Y. Tan, L.P. Tan, F.Y.C. Boey, K.W. Ng, Increasing solvent polarity and addition of salts promote β-phase poly(vinylidene fluoride) formation, Journal of Applied Polymer Science, 128 (2013) 2902-2910.

[44] G.-H. Yang, M. Kim, G. Kim, A hybrid PCL/collagen scaffold consisting of solid freeform-fabricated struts and EHD-direct-jet-processed fibrous threads for tissue regeneration, Journal of Colloid and Interface Science, 450 (2015) 159-167.

[45] L. Vikingsson, B. Claessens, J.A. Gómez-Tejedor, G. Gallego Ferrer, J.L. Gómez Ribelles, Relationship between micro-porosity, water permeability and mechanical behavior in scaffolds

for cartilage engineering, Journal of the Mechanical Behavior of Biomedical Materials, 48 (2015) 60-69.

Figures and Figure Captions

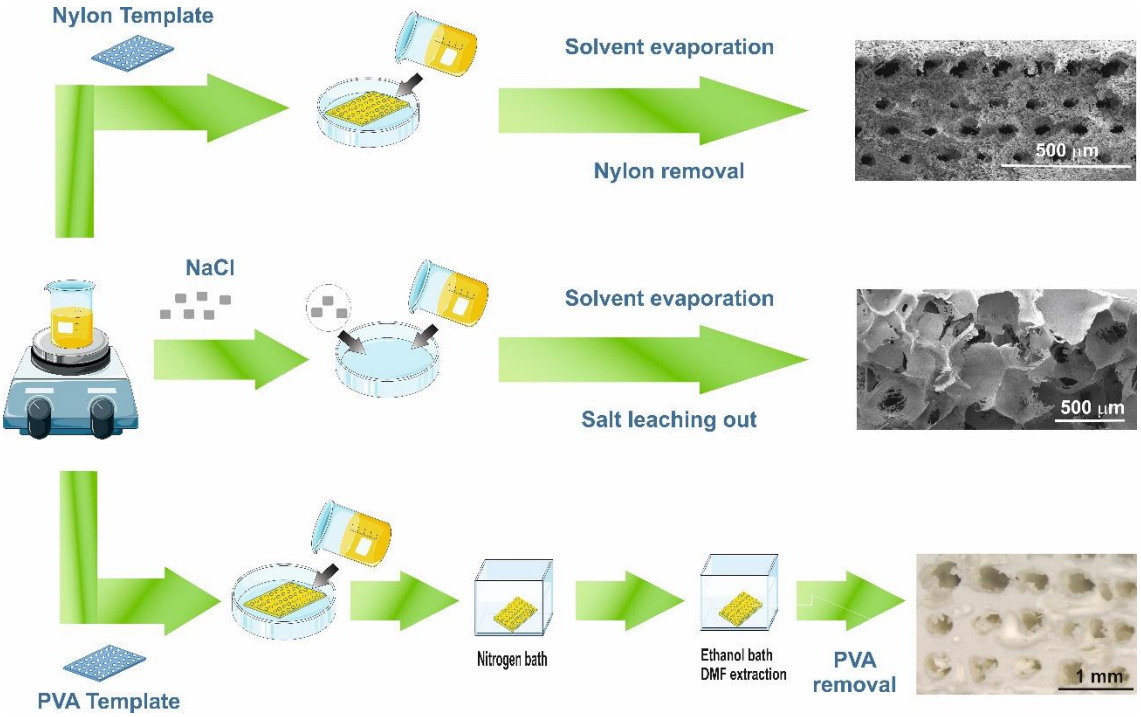

Figure 1. Schematic representation of the different procedures for PVDF three-dimensional scaffolds production.

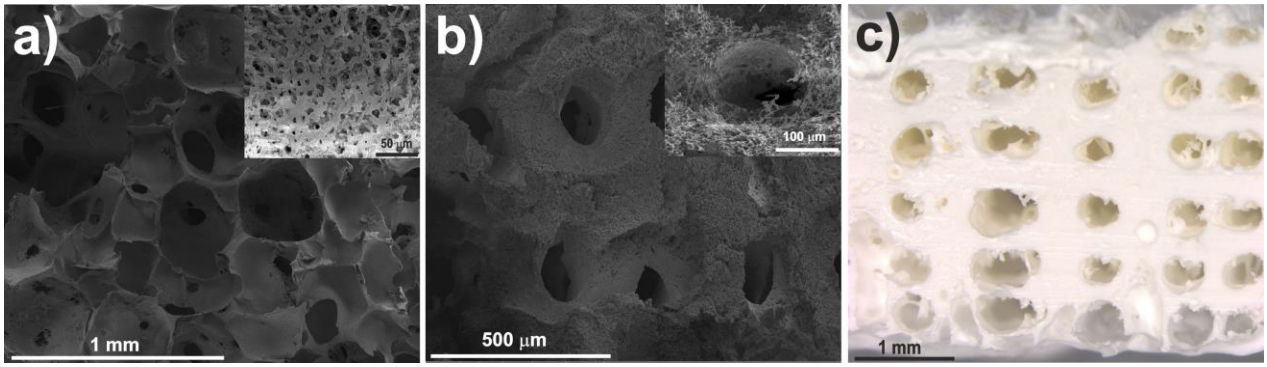

Figure 2. SEM images of the morphology of the PVDF scaffolds obtained by a) salt leaching method, b) using nylon templates and c) using PVA templates and freeze extraction.

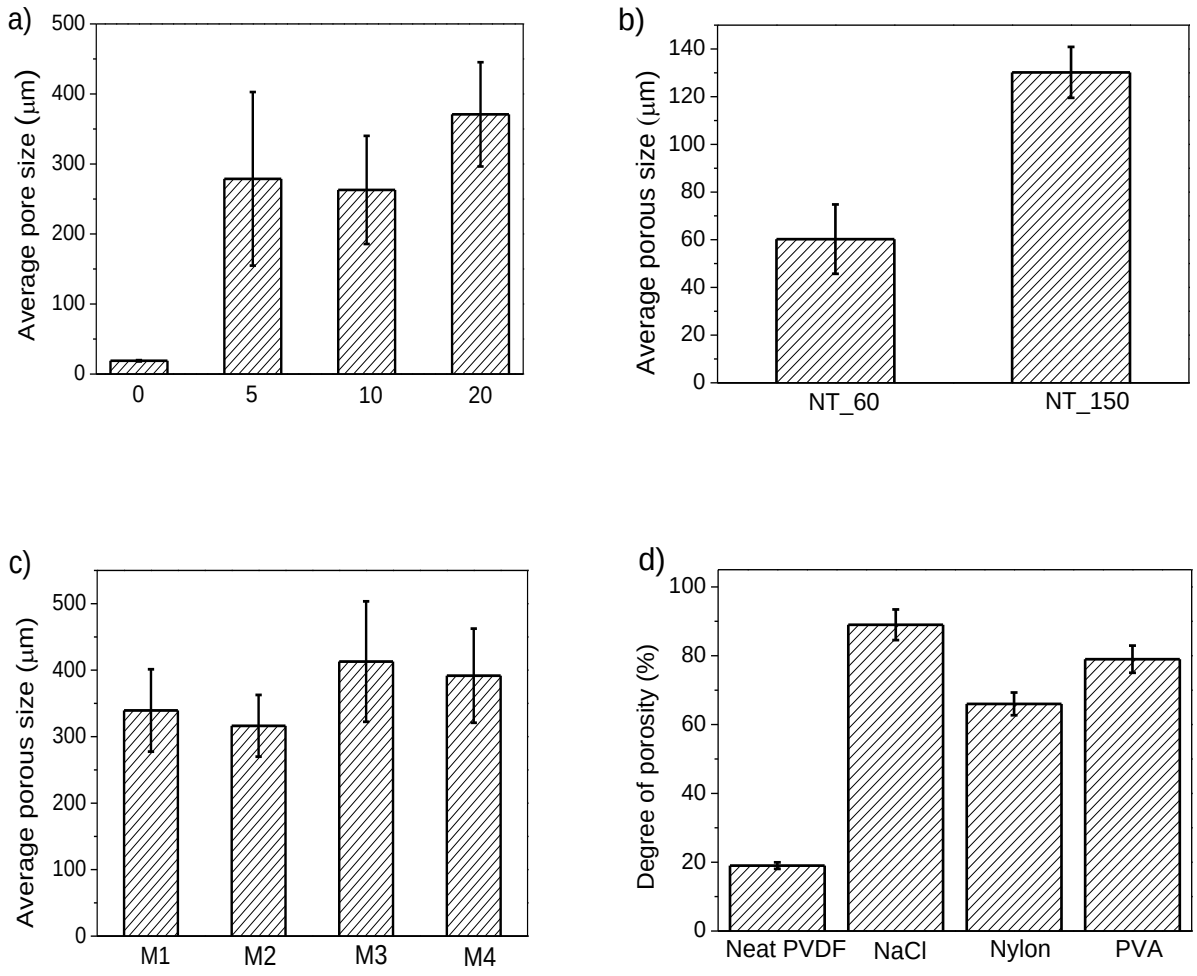

Figure 3. Pore size distribution of the PVDF scaffolds obtained by a) solvent casting with NaCl leaching, b) solvent casting with a 3D nylon template and c) freeze extraction with a 3D PVA template d) Degree of porosity of the PVDF scaffolds.

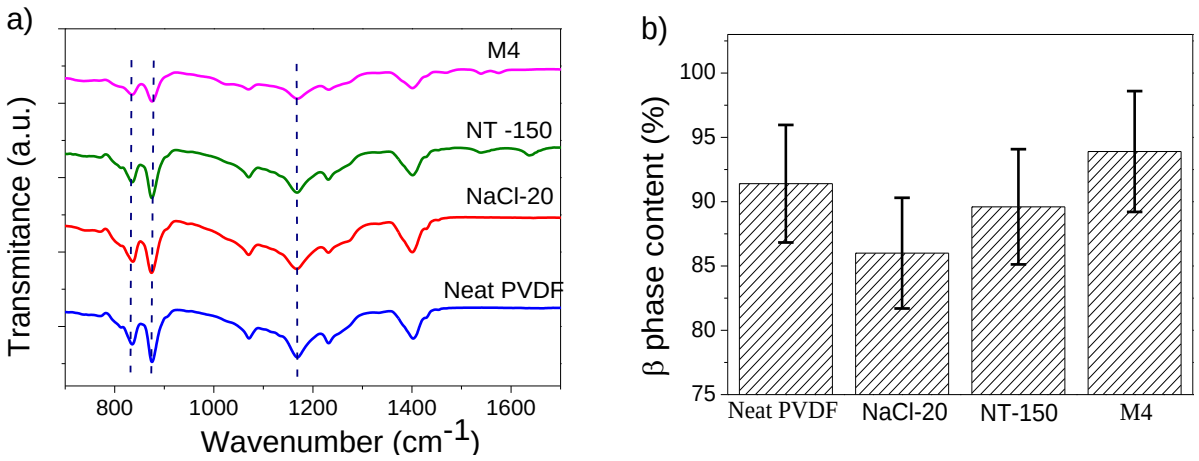

Figure 4. a) FTIR spectra of neat PVDF and the scaffolds processed by different methods and b) variation of β-phase content for the same samples.

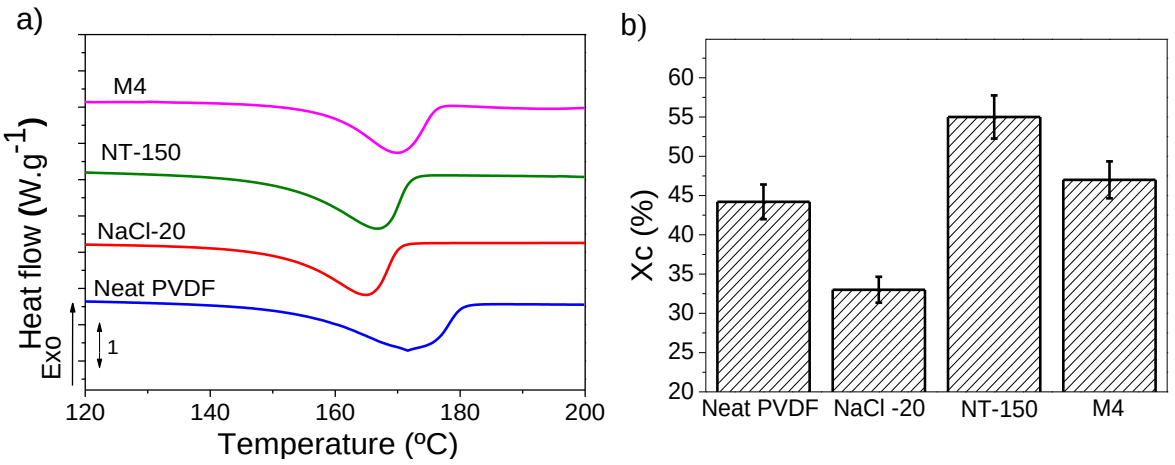

Figure 5. a) DSC thermographs of neat PVDF and PVDF scaffolds obtained from solvent-casting particle leaching and with nylon and PVA templates; b) variation of the degree of crystallinity for the different scaffolds**.**

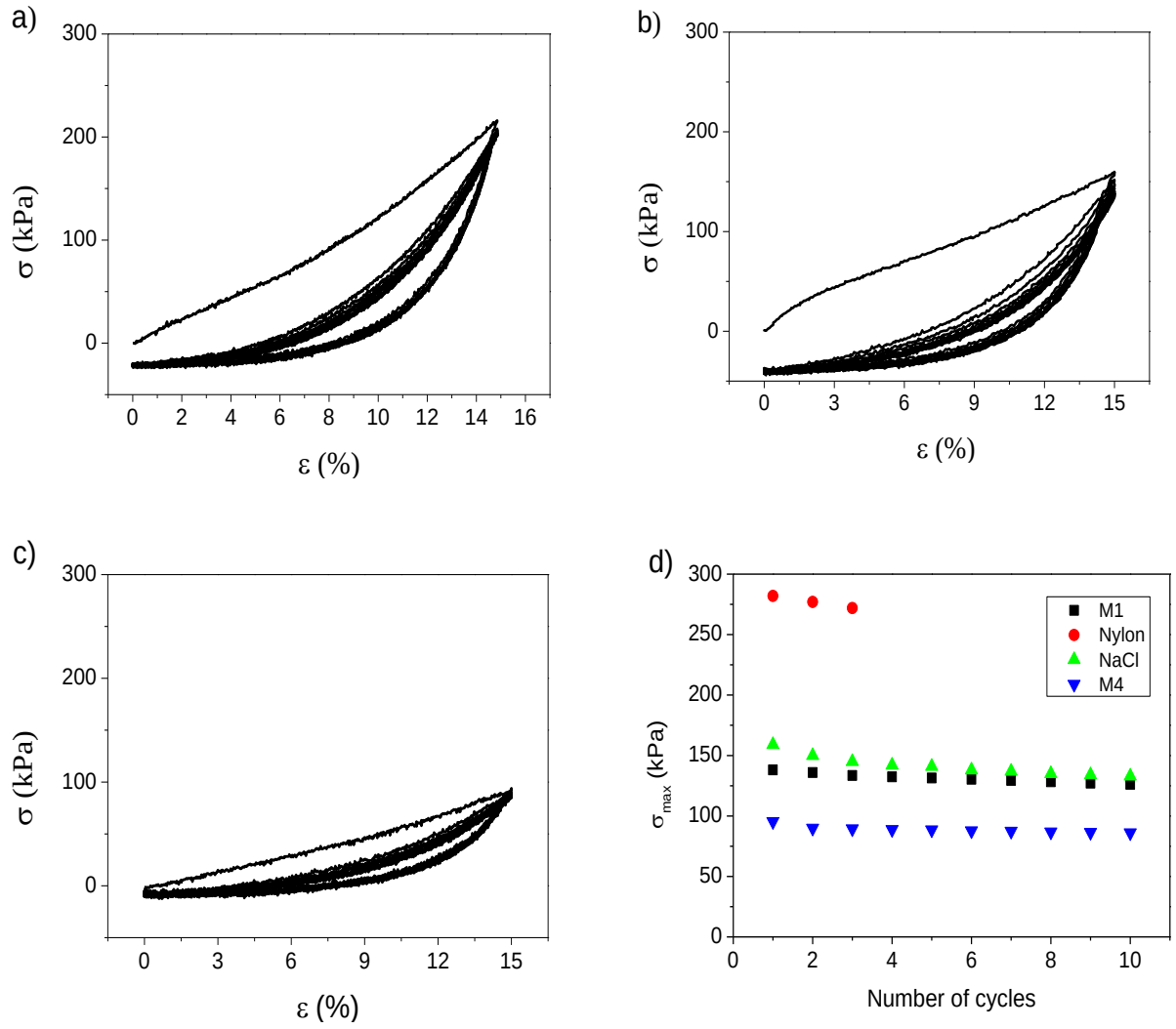

Figure 6. Characteristics stress–strain curves of PVDF scaffolds for compression assays at 15 %. PVDF scaffolds obtained by a) solvent-casting NaCl leaching, b) freeze extraction with a M1 template c) freeze extraction with a M4 template. d) Evolution of the maximum stress obtained up to 10 cycles.

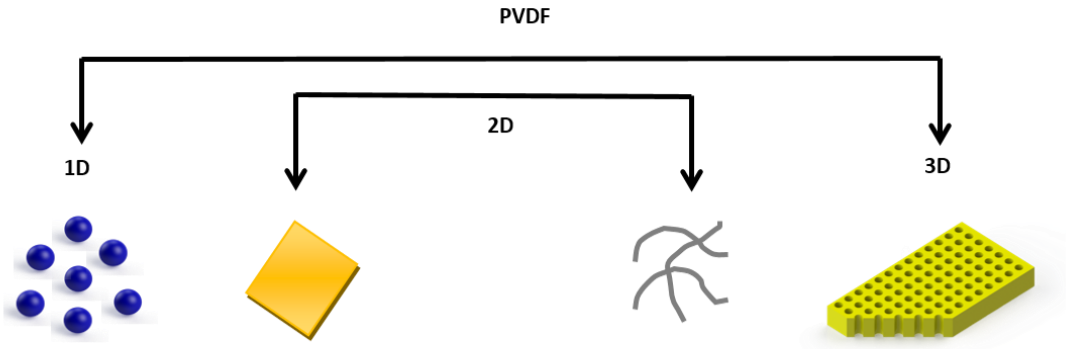

[22] [23] [16, 35, 42] (this study)

Figure 7. Different structures and morphologies of PVDF for tissue engineering applications

Tables and Table Captions

Table 1: PVDF structures, processing method and tissue engineering applications reported in the literature.

Polymeric structure	Composition	Method	Application	Ref.
Particles	PVDF	Electrospray	Tissue engineering	[22]
Films	PVDF	Stretching of α-phase	Fibronectin adsorption	[32]
			Enhanced proliferation of pre-osteoblastic cells	[32]
			Skeletal muscle tissue engineering	[23]
	PVDF	Solution cast	Homogeneous cell distribution and more significant deposition of fibronectin	[33]
Fibers	PVDF	Electrospinning	Skeletal muscle tissue engineering	[23]
			Promoting the neuronal differentiation and neurite extension.	[34]
	PVDF-TrFe	Electrospinning	Promising base material for manipulating cell behavior and proliferation in a three dimensional matrix	[16]
			Neurite extension of primary neurons	[35]
	PVDF/Poly(urethane) (PU)	Electrospinning	Wound healing	[15]
	PVDF	Electrospinning	Bone	[36]

Table 2. PVA template designation with corresponding distance between filaments.

Templates	Filaments distance (mm)
M1	0.6
M2	0.8
M3	1
M4	1.2

Table 3. Tangent modulus (MPa) of scaffolds at 15 % of strain presented as average ± standard deviation**.**

Sample	Young's Modulus (MPa)
NaCl leaching	2.2 ± 0.3
Nylon template	0.4 ± 0.1
M1	0.79 ± 0.08
M2	0.94 ± 0.03
M3	1.02 ± 0.01
M4	1.5 ± 0.3

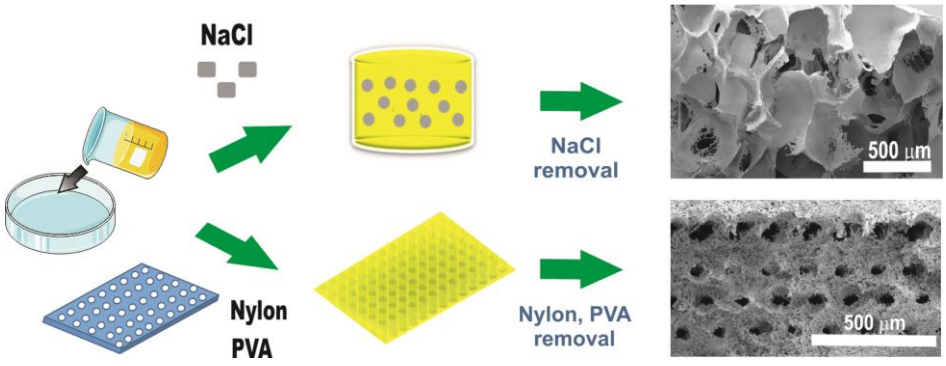
NaCl
NaCl
removal
500 μm
Nylon
PVA
Nylon, PVA
removal
500 μm

Highlights

-Three dimensional scaffolds based on electroactive PVDF have been fabricated.

-Three processing methods, including solvent casting and freeze extraction have been used.

-Different architectures and interconnected porosity have been achieved.

-The scaffolds are in the electroactive β-phase and show a crystallinity degree of ~ 45 %.

-The scaffolds show properties suitable for novel tissue engineering applications.